AIAA Guidance, Navigation, and Control Conference
08 - 11 August 2011, Portland, Oregon

AIAA 2011-6224

Shear Wind Estimation

Ricardo Bencatel[*], João Sousa [†]
School of Engineering, University of Porto, Porto, 4200, Portugal
Mariam Faied[‡] and Anouck Girard[§]
University of Michigan, Ann Arbor, Michigan, MI 48109, USA

This paper presents atmospheric Shear Wind phenomena models and develops a Particle Filter estimator to characterize the phenomena. We describe a model for the Surface Shear Wind and another for the Layer Shear Wind. The models are described and adjusted for Besian estimation. A Particle Filter was implemented and tested in simulation for Surface Shear Wind parameter estimation. The estimator was idealized to be used by small Unmanned Aerial Vehicles (UAVs). The implemented Particle Filter estimates the surrounding flow field with a small number of variables, and as such, low memory requirements.

Nomenclature

$[x, y, z]$	Position vector
$h_{SSW,ref}$	Surface Shear Wind gradient reference altitude
$W_{SSW,ref}$	Surface Shear Wind reference speed
ψ_{SSW}	Surface Shear Wind main direction
$h_{SSW,0}$	Surface Shear Wind *roughness* altitude
$\overline{h}_{LSW}$	Layer Shear Wind mean altitude
Δh_{LSW}	Layer Shear Wind height
$\overline{\mathbf{w}}_{LSW}$	Layer Shear Wind reference velocity
$\Delta \mathbf{w}_{LSW}$	Layer Shear Wind velocity variation

I. Introduction

Small Unmanned Aerial Vehicles (UAVs) are becoming a reference tool by field operatives that need to enhance their situational awareness. However, the desired small size brings together the consequence of reduced energy capacity, either in fuel or battery power. A solution for this problem is to increase their endurance by harvesting energy from atmospheric phenomena.

Shear Wind is the atmospheric phenomenon which occurs on thin layers separating two regions where the predominant air flow vector is different. This difference can be either in speed, in direction, or in both speed and direction. The air layer between these regions is usually less than 100 meters thick, originating a persistent gradient in the flow field. This gradient may be exploited by UAVs[1–4] as it is by birds.[5,6]

The Shear Wind phenomena can be classified by directionality as Vertical or Horizontal Shear. Vertical Shear Wind is a variation of the air flow with altitude. It exists near the ground or water surface,[5,6] on the inversion layer, and on the limits of the jet stream.[7] Surface wind shear is known on the aviation community mainly by its effects on aircraft landing and take-off operations. The reduction of flow speed towards the ground causes the aircraft airspeed to decrease in the same amount, if no compensation is applied. This effect can induce stall, leading to possible catastrophic results. Glider pilots observe Shear Wind sometimes

[*]PhD student, Department of Electrical and Computer Engineering
[†]Invited assistant, Department of Electrical and Computer Engineering
[‡]Post-doc researcher, Department of Aerospace Engineering, 1320 Beal Ave, and AIAA Member
[§]Assistant Professor, Department of Aerospace Engineering, 1320 Beal Ave, and AIAA Life Member

above 3 knots per 1000 feet.[8] Horizontal Shear Wind is a variation of the air flow with a variation with the horizontal position $[x, y]$. It appears across weather fronts and near the coast.

In this work the flow field is the spatial characterization of the air velocity vector. Further, we will refer to the flow field horizontal velocity vector as the wind vector.

I.A. Literature review

The problem of harvesting energy from atmospheric phenomena was addressed by some authors regarding updrafts, Shear Wind and gusts. Allen[9] describes an updraft phenomenon, known as thermals, which is used by glider pilots to remain aloft without a propulsion system. Edwards[10] proved that thermal soaring is feasible with UAVs. He achieved long flights, both in time and flown distance, at several different flight sites. Langelaan[4] describes how gusts affect aircraft and how flight controllers can lead the aircraft to loose or gain energy with gusts. Lawrance and Sukkarieh[1–3] presented energy based methods for soaring path planning. The first work describes a method suitable for static and dynamic soaring, i.e., both in thermals and shear flow fields. The second work describes a promising controller for Shear Wind soaring. The third work describes a path planner to simultaneously acquire information about the surrounding flow field and explore the available flow energy. Sachs[5] describes how birds and aircraft can harvest energy from surface Shear Wind. He also determines the bound conditions for perpetual flight with this phenomenon. Sachs et al.[6] studied Albatross real flight paths while these were take advantage of the Surface Shear Wind.

I.B. General problem

As described before, energy harvest from Shear Wind phenomena should be feasible. We will focus on Vertical Shear Wind, as surface, inversion, and jet stream shear are quite steady phenomena. Birds learn how to use these phenomena. UAVs may be programmed to do the same. The main requirements are: knowing the phenomenon characteristics and control the aircraft to execute an energy harvesting flight path. The control methods developed by Lawrance and Sukkarieh[1–3] required knowledge of the surrounding flow field. These phenomena occur over large areas, which makes it difficult to characterize as a whole. Lawrance and Sukkarieh's solution for this characterization is a Gaussian Progress (GP) regression that describes the flow field over spatially distributed points.

I.C. Current approach

Our approach is a model-based estimation, requiring few characterization parameters. As such, we simplify the phenomena to uniaxial (z) wind vector variations, i.e., define the wind vector as a function of the altitude only. We further distinguish the Vertical Shear Wind phenomena in Surface and Layer Shear Wind, as the flow gradient is different for each phenomena. We will describe both phenomena modelling functions and the sensing method in section II.

To estimate the characterizing parameters we developed a Particle Filter. Particle Filters handle well the phenomena nonlinearities and may be extended to simultaneously localize several different Shear Wind layers. In section III we define the propagation and observation models and estimations method.

The results and conclusions are described in sections IV and V.

II. Models

II.A. Surface Shear Wind

Surface Shear Wind is a special case of vertical shear where instead of two air mass regions we have one air mass region and a surface. The surface is usually still or moving at very low speeds relatively to the general air mass, as is the case of water surfaces. The Shear Wind layer starts at the ground level and may be modeled by:[5,11]

$$W_H = W_{H_{ref}} \frac{\ln(h/h_0)}{\ln(h_{ref}/h_0)}, \tag{1}$$

where W_H is the total wind speed and $W_{H_{ref}}$, h_{ref}, and h_0 are reference values. $W_{H_{ref}}$ is the reference wind speed at an altitude h_{ref} away from the surface. h_0 defines the shape of the flow gradient, reflecting the

surface properties, like irregularity, roughness and drag. In the Military Specification MIL-F-8785C:[11]

$$h_{ref} = 6m$$
$$h_0 = \begin{cases} 0.15 & for\ Category\ C\ flight\ phases \\ 2.0 & otherwise \end{cases}, \tag{2}$$

if $1m \leq h \leq 300m$. Category C flight phases are the terminal flight phases, which include takeoff, approach, and landing, as defined in reference.[11]

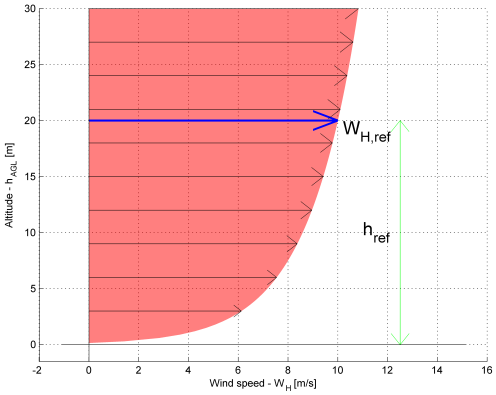

Figure 1: Surface wind shear profile

II.B. Layer Shear Wind

We present a simple model for the layer wind shear. We approximate de wind gradient with a gaussian. This results in a wind speed profile as the illustrated in figure 2a and modeled by:

$$\mathbf{w}_{H,h_{UAV}} = \mathbf{w}_{H,LSW,h_{min}} + \frac{\Delta \mathbf{w}_{H,LSW}}{2}\left[1 + \mathrm{erf}\left(4\frac{h_{UAV} - \overline{h}_{LSW}}{\Delta h_{LSW}}\right)\right], \tag{3}$$

where h_{min} and h_{max} are the wind shear layer limit altitudes, $\mathbf{w}_{H,LSW,h}$ is the wind vector due to the wind shear phenomenon at an altitude h, and:

$$\Delta \mathbf{w}_{H,LSW} = \mathbf{w}_{H,LSW,h_{max}} - \mathbf{w}_{H,LSW,h_{min}} \tag{4a}$$
$$\overline{h}_{LSW} = \frac{h_{max} + h_{min}}{2} \tag{4b}$$
$$\Delta h_{LSW} = h_{max} - h_{min}. \tag{4c}$$

The wind gradient is illustrated on figure 2b and modeled by:

$$\left.\frac{\delta \mathbf{w}_{LSW}}{\delta h}\right|_{h_{UAV}} = \frac{4\left\|\Delta \mathbf{w}_{LSW}\right\|}{\Delta h_{LSW}\sqrt{\pi}} e^{-\left(4\frac{h_{UAV} - \overline{h}_{LSW}}{\Delta h_{LSW}}\right)^2}, \tag{5}$$

II.C. UAV sensing

The UAV is affected by the air flow. As such, it may estimate the flow field state through its sensors measurements. This estimate is usually obtained through a flow field observer. If we regard the UAV with its sensors and a flow field observer as a single system, this can now be considered as a sensor for the Shear Wind phenomena.

In this work, the relevant UAV measurements are the local wind vector $\mathbf{w}$ and the position vector $\mathbf{p}_{UAV} = [x_{UAV}, y_{UAV}, h_{UAV}]$, where h_{UAV} is the altitude above ground level. It is assumed the UAV can estimate its position with good enough accuracy to take it as ground truth for the Shear Wind locator.

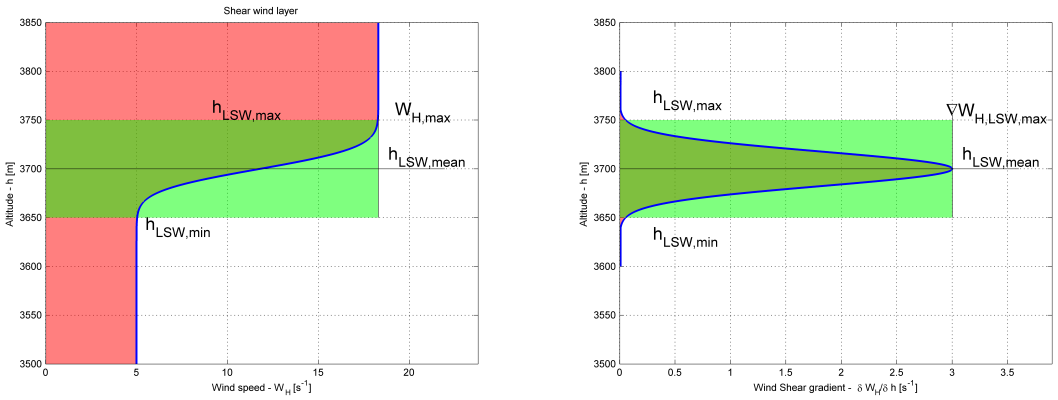

(a) Layer wind shear profile

(b) Layer wind shear gradient

Figure 2: Variation of wind speed over a Shear Wind layer

III. Shear Wind localization

III.A. Shear Wind propagation models

III.A.1. Surface Shear Wind

The surface Shear Wind state vector is $\mathbf{x}_{SSW} = [W_{SSW,6}, \psi_{SSW}, h_{SSW,0}]^\intercal$, where $W_{SSW,6}$ is the wind speed at 6 meters above ground level due to the surface Shear Wind, as specified in the Military Specification MIL-F-8785C.[11] ψ_{SSW} is the surface Shear Wind main direction, which we assume constant from the ground level to the reference altitude, 6 meters in this case. $h_{SSW,0}$ is *roughness* altitude, which defines the surface Shear Wind gradient shape. The gradient dynamics are described by:

$$\dot{\mathbf{x}}_{SSW} = \varepsilon_{SSW}, \tag{6}$$

where ε_{SSW} is a disturbance vector. The dynamics can be discretized in time, yielding

$$\mathbf{x}_{SSW,t} = \mathbf{x}_{SSW,t-1} + \varepsilon_{SSW}, \tag{7}$$

with $\varepsilon_{SSW} \sim \mathcal{N}\left(0, \left[\delta^2_{W_{SSW,6}}, \delta^2_{\psi_{SSW}}, \delta^2_{h_{SSW,0}}\right]^\intercal\right)$ and $\delta_{(\cdot)}$ are the horizontal wind velocity, the Shear Wind direction, and *roughness* altitude rates of change, respectively. This rates of change account for the parameters time variation and for the spacial variation of the aircraft position.

An alternative propagation model for the surface Shear Wind is one which allows the altitude reference to vary from the one specified in the MIL-F-8785C.[11] The state vector would then be $\mathbf{x}_{SSW} = [h_{SSW,ref}, W_{SSW,ref}, \psi_{SSW}, h_{SSW,0}]^\intercal$, where $h_{SSW,ref}$ is the gradient reference altitude, $W_{SSW,ref}$ is the average horizontal wind velocity at $h_{SSW,ref}$, ψ_{SSW} is the surface Shear Wind main direction, and $h_{SSW,0}$ is *roughness* altitude. The gradient dynamics are now described by:

$$h_{SSW,ref,t} = h_{SSW,ref,t-1} + \varepsilon_{h_{SSW,ref}} \tag{8a}$$

$$W_{SSW,ref,t} = W_{SSW,ref,t-1} \frac{\ln\left(h_{SSW,ref,t}/h_{SSW,0,t-1}\right)}{\ln\left(h_{SSW,ref,t-1}/h_{SSW,0,t-1}\right)} + \varepsilon_{W_{SSW,ref}} \tag{8b}$$

$$\psi_{SSW} = \psi_{SSW,t-1} + \varepsilon_{\psi_{SSW}} \tag{8c}$$

$$h_{SSW,0,t} = h_{SSW,0,t-1} + \varepsilon_{h_{SSW,0}} \tag{8d}$$

$$\tag{8e}$$

with $\varepsilon_{h_{SSW,ref}} \sim \mathcal{N}\left(0, \delta^2_{h_{SSW,ref}}\right)$, $\varepsilon_{W_{SSW,ref}} \sim \mathcal{N}\left(0, \delta^2_{W_{SSW,ref}}\right)$, $\varepsilon_{\psi_{SSW}} \sim \mathcal{N}\left(0, \delta^2_{\psi_{SSW}}\right)$, and $\varepsilon_{h_{SSW,0}} \sim \mathcal{N}\left(0, \delta^2_{h_{SSW,0}}\right)$. $\delta_{(\cdot)}$ are the surface Shear Wind reference altitude, the horizontal wind velocity, the Shear Wind direction, and the *roughness* altitude rates of change, respectively.

III.A.2. Layer Shear Wind

The layer Shear Wind state vector is $\mathbf{x}_{LSW} = \left[\overline{h}_{LSW}, \Delta h_{LSW}, \overline{\mathbf{w}}_{LSW}, \Delta \mathbf{w}_{LSW}\right]^{\mathsf{T}}$, where $\overline{h}_{LSW}$ is the mean altitude of the Shear Wind layer, Δh_{LSW} is Shear Wind layer height, $\overline{\mathbf{w}}_{LSW}$ and $\Delta \mathbf{w}_{LSW}$ are the horizontal wind vector mean and variation over the Shear Wind layer. As with the surface Shear Wind, this is only a correct representation of the layer Shear Wind if we assume a constant wind gradient direction. The gradient dynamics are described by:

$$\dot{\mathbf{x}}_{LSW} = \varepsilon_{LSW}, \tag{9}$$

where ε_{LSW} is a disturbance vector. The dynamics can be discretized in time, yielding

$$\mathbf{x}_{LSW,t} = \mathbf{x}_{LSW,t-1} + \varepsilon_{LSW}, \tag{10}$$

with $\varepsilon_{LSW} \sim \mathcal{N}\left(0, \left[\delta^2_{\overline{h}_{LSW}}, \delta^2_{\Delta h_{LSW}}, \delta^2_{\mu_{W,LSW}}{}^{\mathsf{T}}, \delta^2_{\Delta W_{LSW}}{}^{\mathsf{T}}\right]^{\mathsf{T}}\right)$ and $\delta_{(\cdot)}$ are the rates of change of the all layer Shear Wind state parameters, respectively. As with the surface Shear Wind parameters, this rates of change account for the parameters time variation and the change with spacial variation of the aircraft position.

III.B. Shear Wind observation models

The horizontal wind vector observation ($\mathbf{w}_H$) may be described by

$$\mathbf{w}_H = [W_x, W_y]^{\mathsf{T}} \approx \mathbf{h}\left(\mathbf{x}_{SW}, \mathbf{p}_{UAV}\right) + \varepsilon_{W_H}, \tag{11}$$

where W_x and W_y are estimated with a wind observer.

The observation uncertainty (ε_{W_H}) is caused mainly by gusts, but also by the UAV sensing noise, i.e., the wind observer errors. As such, it may be defined as:

$$\varepsilon_{W_H} = \varepsilon_{W_H,Gust} + \varepsilon_{W_H,Sens} \tag{12a}$$

$$\varepsilon_{W_H,Gust} \sim N\left(0, k_{Gust} \cdot \hat{\overline{\mathbf{w}}}_H\right) \tag{12b}$$

$$\varepsilon_{W_H,Sens} \sim N\left(0, \sigma_{WObs}\right), \tag{12c}$$

where k_{Gust} is an adimensional ratio relating the wind variation with the wind average:

$$k_{Gust} = \frac{\sqrt{\mathsf{E}\left[\left(\overline{\|\mathbf{w}_H\|} - \|\mathbf{w}_H\|\right)^2\right]}}{\overline{\|\mathbf{w}_H\|}}, \tag{13}$$

$\hat{\overline{\mathbf{w}}}_H$ is the estimate of the average horizontal wind, and σ_{WObs} is the wind observer uncertainty vector.

III.B.1. Surface Shear Wind

The surface Shear Wind observation model is derived from (1):

$$\hat{\overline{\mathbf{w}}}_H = \mathbf{h}\left(\mathbf{x}_{SSW}, \mathbf{p}_{UAV}\right) = W_{SSW,ref} \frac{\ln\left(h_{UAV}/h_{SSW,0}\right)}{\ln\left(h_{SSW,ref}/h_{SSW,0}\right)} \begin{bmatrix} \cos\psi_{SSW} \\ \sin\psi_{SSW} \end{bmatrix}. \tag{14}$$

III.B.2. Layer shear

The layer Shear Wind observation model is derived from (15):

$$\hat{\overline{\mathbf{w}}}_H = \mathbf{h}\left(\mathbf{x}_{LSW}, \mathbf{p}_{UAV}\right) = \mathbf{w}_{h_{min},LSW} + \frac{\Delta \mathbf{w}_{LSW}}{2}\left[1 + \operatorname{erf}\left(4\frac{h_{UAV} - \overline{h}_{LSW}}{\Delta h_{LSW}}\right)\right], \tag{15}$$

where $\mathbf{w}_{h_{min},LSW} = \overline{\mathbf{w}}_{LSW} - \frac{\Delta \mathbf{w}_{LSW}}{2}$.

III.C. Inference framework

In this work, the estimation is implemented through a Particle Filter. The belief distribution at each estimation step is represented by particles defined by the state vector $\mathbf{x}_{SSW}$ or $\mathbf{x}_{LSW}$. Each particle is an hypothesis of the current state. At each step, particles are propagated, evaluated and resampled, to create a new estimate. The particles are propagated through the propagation model described in section III.A. This step allows the filter to track the state evolution and represent the uncertainty. The observation model, presented in section III.B, generates the expected observation for each particle. This is combined with the UAV observation to provide a measurement of likelihood of the hypothesis represented by each particle. The resampling prunes the unlikely particles (hypothesis).

III.D. Particle generation

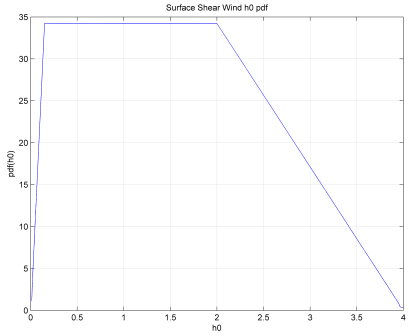

Figure 3: Surface Shear Wind "roughness" altitude distribution generated

III.D.1. Surface Shear Wind

The estimation particles are generated when the UAV is low enough to measure the effect of the Surface Shear Wind. The current application of Particle Filter assumes a fixed reference altitude as specified in MIL-F-8785C.[11] The generated particles represent distribution of the "roughness" altitude as illustrated in figure 3. The reference wind vector distribution is centered on the current wind measurement adjusted for the reference altitude (1), with a Gaussian distribution. Figure 4 illustrates the typical particle generation distribution, in terms of wind vector.

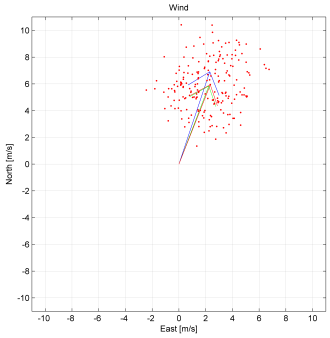

Figure 4: Particle generation

IV. Results

The results presented next were obtained through multiple simulation of UAV flights sweeping Shear Wind phenomena. The UAV was simulated by an extended unicycle model, which included altitude variations. In the simulation the UAV is commanded to sweep a range of altitudes, including those affected by Shear Wind

phenomena. The wind simulation summed the Shear Wind effects to gusts. The gusts were generated by a scalar Gauss-Markov process, which simulates well the kind of sensing noise the system would be subject to in reality.

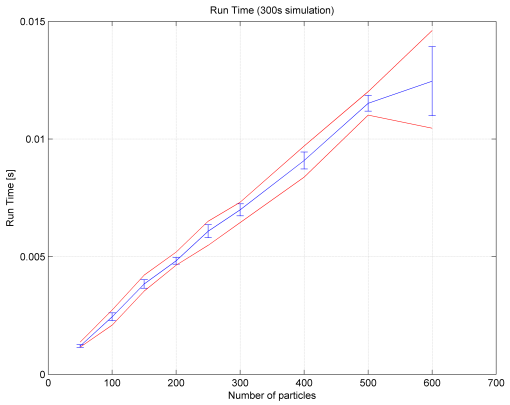

Figure 5: Surface Shear Wind Particle Filter cycle run time with the number of estimation particles.

We run the 20 independent simulations with each particle quantity choice to characterize statistically the developed Particle Filters. As expected the time required by the Particle Filter for each estimation cycle grows almost linearly with the number of particles (fig. 5). However the estimation quality doesn't improve linearly with the number of particles. In fact, for the Surface Shear Wind the estimation quality is almost the same for 200 estimation particles or more (fig. 6). In MatLab®, on a Intel® Core™2 Duo CPU, T9300 @ 2.5GHz, a Particle Filter estimation cycle takes less then $5 \times 10^{-30} s$. Further, the Particle Filter doesn't need to run at more than 5Hz to obtain good quality estimations. This means that this Particle Filter with 200 particles can run in real time, with almost no extra load to the processor, and good quality estimates.

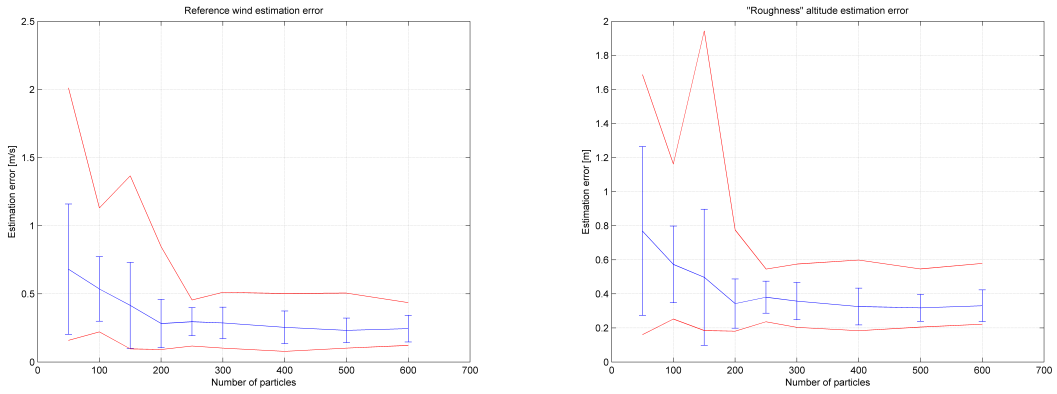

(a) Reference wind vector estimation error

(b) "Roughness" altitude estimation error

Figure 6: Surface Shear Wind parameters estimation error as a function of the number of particles in particle filter.

The average wind prediction error (fig. 7) is mostly under half a meter per second. This error is mostly due to the gusts, as the filter is estimating the effect of the steady Shear Wind and not the gusts.

V. Conclusion

A regular Particle Filter with 200 particles is well suited for real time estimation of Surface Shear Wind parameters. We were able to estimate and track the Surface Shear Wind effects using a Particle Filter with only three parameters. This avoids the need to maintain a time history of the observed flow field or a

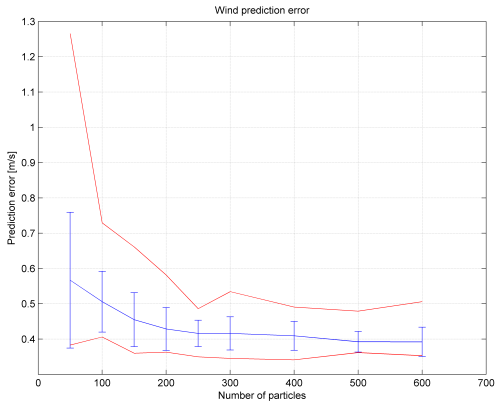

Figure 7: Wind prediction error of Surface Shear Wind Particle Filter with the number of estimation particles.

spatially distributed characterization of it.

V.A. Future Work

We will test the Layer Shear Wind estimator in the near future and expect to obtain results very similar to the Surface Shear Wind one. We'll also couple this methods with a wind observer and test them on real UAV flights. This should validate not only the methods, but also the atmospheric phenomena models on which they were based. Further, we intend to use the estimates to feed a flight controller to take advantage of the Shear Wind and improve UAVs' endurance.

Acknowledgments

We gratefully acknowledge the support of the AsasF group and the researchers from the Underwater Systems and Technology Laboratory, specially Gil Gonçálves, Eduardo Oliveira, Rui Caldeira, and Filipe Ferreira, and the Portuguese Air Force Academy, specially Cap. Elói Pereira and Lt. Tiago Oliveira. The research leading to this work was funded by Financiamento pluri-anual of the FEUP ISR Porto R&D unit and by the FCT (Foundation for Science and Technology) under PhD grant SFRH/BD/40764/2007.

References

[1]Lawrance, N. R. and Sukkarieh, S., "Wind Energy Based Path Planning for a Small Gliding Unmanned Aerial Vehicle," *AIAA Guidance, Navigation, and Control Conference*, AIAA, Chicago, Illinois, Aug. 10-13 2009.

[2]Lawrance, N. R. J. and Sukkarieh, S., "A guidance and control strategy for dynamic soaring with a gliding UAV," *Robotics and Automation, 2009. ICRA '09. IEEE International Conference on*, may 2009, pp. 3632 –3637.

[3]Lawrance, N. R. and Sukkarieh, S., "Simultaneous Exploration and Exploitation of a Wind Field for a Small Gliding UAV," *AIAA Guidance, Navigation, and Control Conference*, Toronto, Ontario, Canada, Aug. 2-5 2010.

[4]Langelaan, J., "Gust Energy Extraction for Mini and Micro Uninhabited Aerial Vehicles," *Journal of Guidance, Control, and Dynamics*, Vol. 32, No. 2, July-August 2009, pp. 464–473.

[5]Sachs, G., "Minimum shear wind strength required for dynamic soaring of albatrosses," *Ibis - The International Journal of Avian Science*, Vol. 147, No. 1, 2005, pp. 1–10.

[6]Sachs, G., Traugott, J., and Holzapfel, F., "In-Flight Measurement of Dynamic Soaring in Albatrosses," *AIAA Guidance, Navigation, and Control Conference*, Toronto, Ontario, Canada, Aug. 2-5 2010.

[7]Grenestedt, J. L. and Spletzer, J. R., "Optimal Energy Extraction During Dynamic Jet Stream Soaring," *AIAA Guidance, Navigation, and Control Conference*, Toronto, Ontario, Canada, Aug. 2-5 2010.

[8]FAA, *Aviation Weather*, Aviation Supplies & Academics, Inc., October 1 1975.

[9]Allen, M. J., "Updraft Model for Development of Autonomous Soaring Uninhabited Air Vehicles," *44rd AIAA Aerospace Sciences Meeting and Exhibit*, AIAA, Reno, Nevada, 9 - 12 January 2006.

[10]Edwards, D. J., "Implementation Details and Flight Test Results of an Autonomous Soaring Controller," *AIAA Guidance, Navigation, and Control Conference*, AIAA, Honolulu, Hawaii, Aug. 10-13 2008.

[11] *U.S. Military Specification MIL-F-8785C*, 5 November 1980.